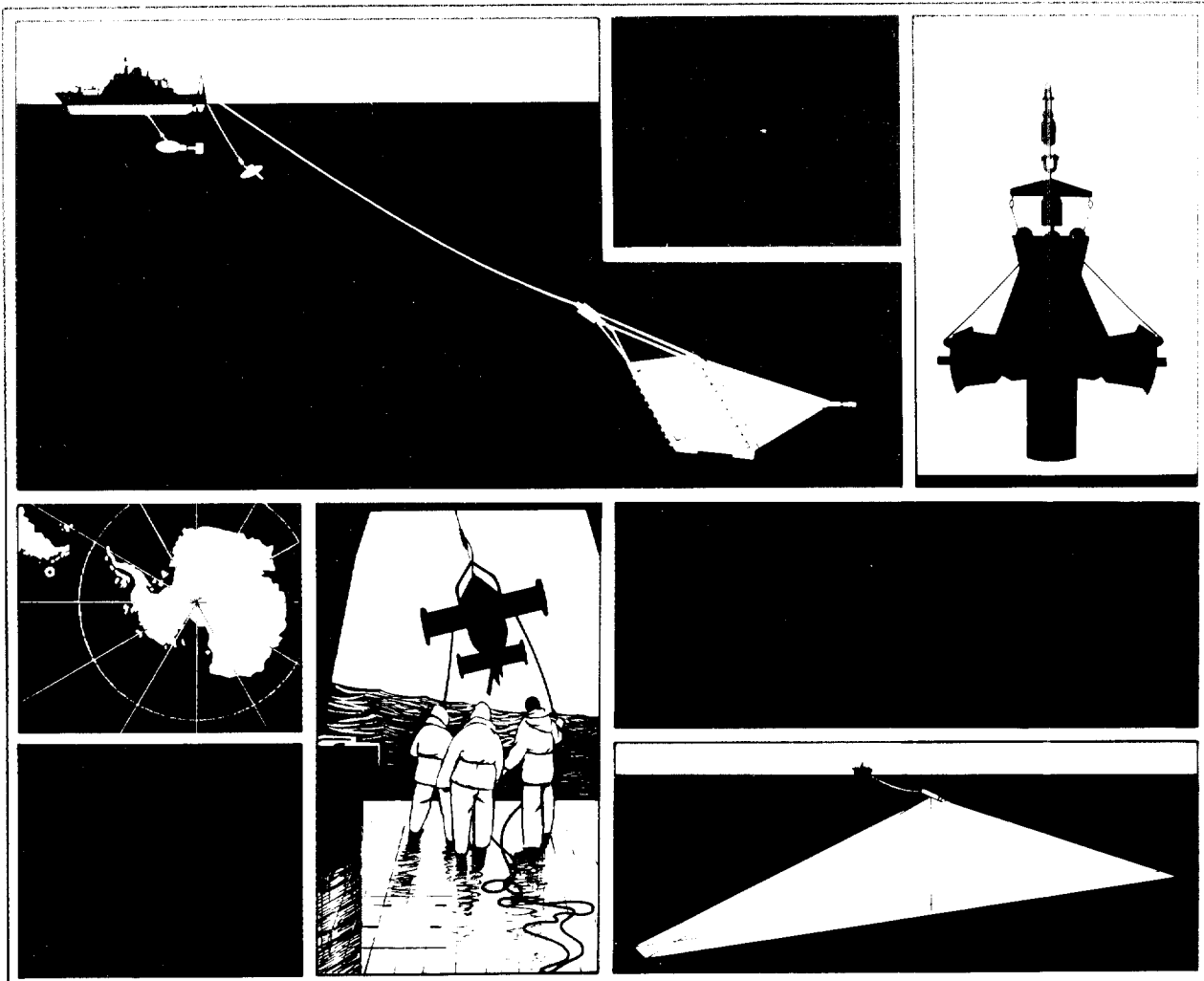




# The IOSDL SeaSoar hydraulic unit: laboratory test report

T J P Gwilliam, D Grohmann & R F Wallace

Report No 300 1992



**INSTITUTE OF OCEANOGRAPHIC SCIENCES  
DEACON LABORATORY**

---

**Wormley, Godalming,  
Surrey, GU8 5UB, U.K.**

**Telephone: 0428 79 4141  
Telex: 858833 OCEANS G  
Telefax: 0428 79 3066**

Director: Dr. C.P. Summerhayes

**INSTITUTE OF OCEANOGRAPHIC SCIENCES**

**DEACON LABORATORY**

**REPORT NO. 300**

The IOSDL SeaSoar hydraulic unit:  
laboratory test report

T J P Gwilliam, D Grohmann & R F Wallace

1992



# DOCUMENT DATA SHEET

<i>AUTHOR</i> G WILLIAM, T J P, GROHMANN, D & WALLACE, R F	<i>PUBLICATION DATE</i> 1992
<i>TITLE</i>  The IOSDL SeaSoar hydraulic unit: laboratory test report.	
<i>REFERENCE</i>  Institute of Oceanographic Sciences Deacon Laboratory, Report, No. 300, 37pp.	
<i>ABSTRACT</i>  <p>This is a report on a series of static and dynamic laboratory measurements taken on five SeaSoar hydraulic units. It fully describes their operation, the test equipment and the test methods used.</p> <p>Analysis of the test results provide power efficiency and loss information for each unit. An estimate of the input on output torque requirements at peak load conditions is also included.</p>	
<i>KEYWORDS</i>  SEASOAR	
<i>ISSUING ORGANISATION</i>  <p>Institute of Oceanographic Sciences Deacon Laboratory Wormley, Godalming Surrey GU8 5UB. UK.</p> <p>Director: Colin Summerhayes DSc</p> <p>Telephone Wormley (0428) 684141 Telex 858833 OCEANS G. Facsimile (0428) 683066</p>	
Copies of this report are available from: <b>The Library,</b> <i>PRICE</i> <b>£13.00</b>	



<b>CONTENTS</b>	<b>Page</b>
<b>INTRODUCTION</b>	7
<b>HYDRAULIC UNIT</b>	7
<b>General Description</b>	7
<b>Preparation</b>	8
<b>TEST EQUIPMENT REQUIREMENTS</b>	8
<b>TESTING PROGRAMME. PROCEDURES AND RESULTS</b>	9
<b>Testing Programme</b>	9
<b>Procedures and Results</b>	9
<b>Motor Losses</b>	9
<b>End Plate Load Test</b>	10
<b>Spring Load Test</b>	11
<b>Hydraulic Unit No. 1 Performance Calculations</b>	12
<b>ANALYSIS</b>	18
<b>Push and Pull Force Differences</b>	18
<b>Power Losses</b>	20
<b>Input and Output Torque Calculations</b>	21
<b>Oil Leakage Problems</b>	22
<b>CONCLUSIONS</b>	23
<b>ACKNOWLEDGEMENTS</b>	23
<b>APPENDICES</b>	
<b>A SeaSear Hydraulic Unit Preparation Procedure</b>	24
<b>B Abbreviations used in this Report</b>	25

**DIAGRAMS AND TABLES**

<b>Figure No.</b>	<b>Title</b>	<b>Page No.</b>
1	SeaSoar Hydraulic Circuit	26
2	SeaSoar Hydraulic Unit Test Bench	27
3	SeaSoar Hydraulic Unit Test Rig. Cycling Circuit	28
4	D.C. Motor off Load Speed Related Losses	29
5	Unit No.1 End plate Test	30
6	Unit No.2 End plate Test	31
7	Unit No.3 End plate Test	32
8	Unit No.1 Push Mode	33
9	Unit No.2 Push Mode	33
10	Unit No.3 Push Mode	34
11	Unit No.4 Push Mode	34
12	Unit No.5 Push Mode	35
13	Unit No.1 Pull Mode	35
14	Unit No.2 Pull Mode	36
15	Unit No.3 Pull Mode	36
16	Unit No.4 Pull Mode	37
17	Unit No.5 Pull Mode	37
18	Spring Work Diagram	13
19	Ram to Wing Linkage	21
Table 1	Push Mode spring test data	16
Table 2	Pull Mode spring test data	17
Table 3	End Plate test data	19



## **1.0 INTRODUCTION**

This report describes a series of measurements carried out on the IOSDL SeaSoar hydraulic units as part of an on-going inspection of the whole SeaSoar system. Development work on the current series of hydraulic units was first carried out in 1977 by R. Dobson at IOSDL and although development work on components has continued up to the present time, the unit remains very much in its original form.

The primary aim of these particular tests is to advance our working knowledge of the instrument so that further improvements can be made to their operational performance and reliability. It is also hoped that the knowledge gained from these tests can be used for two further studies. The first, to reduce the physical size of the existing instrument and the second, to find an alternative method of wing control.

## **2.0 HYDRAULIC UNIT**

### **2.1. General Description**

The hydraulic unit is housed in a 388 mm long, 114.3 mm outside diameter stainless steel tube which is mounted in the tail section of the SeaSoar vehicle where it provides the power necessary to move the wings through a 30 degree range.

At one end of the hydraulic tube, and projecting outside and to the rear of the vehicle, is a six bladed impeller which rotates as the ship tows the vehicle through the water. The impeller shaft is coupled via bearings and seals to the hydraulic gear pump, mounted inside the tube, which provides the necessary oil pressure to operate a piston ram assembly. Measurements taken under operational conditions indicate that impeller revolutions of between 150 and 200 revolutions per minute (rpm) are normal for ship speeds between 8 and 9 knots.

Fig. 1 is a schematic diagram which illustrates the essential components of the hydraulic circuit. The high pressure (HP) oil flow from the gear pump is first filtered before passing to the bi-directional control valve which is a standard Moog unit, type E030-018. The direction of the oil flow to the piston/ram assembly is controlled by two solenoid valves mounted within the unit. The direction of the flow, and hence the direction of wing movement, is controlled by the polarity of the signal from the current driver in the servo-amplifier of the shipboard control system. The amplitude of the signal controls the flow of oil through the valve to the piston, which is therefore controlling the response time of the system. Signal levels of 5milli-amps are sufficient to fully open the valves to provide maximum flow. The return low pressure (LP) line to the gear pump incorporates a filter and oil reservoir, the latter providing a means of pressure balancing the unit as well as making up for the changes in cylinder volume with piston position.

To reduce the effects of wear and corrosion, the ram has chrome hardened surfaces where it projects through the tube end cap, while shaft seals and a bellows assembly protect the internal mechanism from the ingress of water. Adjustable linkages connect the ram to the wing assembly, converting the 60 mm linear movement of the ram to a 30 degree (0.52 radian) rotational movement of the wing.

## **2.2 Preparation**

Initially, it was expected that only the three IOSDL units would be available for testing but an opportunity arose to include two further units in later tests. Prior to testing, all the units were given a general overhaul and a standard IOSDL pre-cruise check-out similar to that listed in appendix B.

## **3.0 TEST EQUIPMENT REQUIREMENTS**

In preparing the programme of measurements to assess the performance of the hydraulic unit, it became obvious that a custom built test rig was required to handle the tensile and compressive forces of 1000kgf (9806N).

The diagram of fig.2 is a side view presentation of the rig together with its major dimensions. The bench is of welded construction, using 38mm drawn square section mild steel. The hydraulic unit under test can be mounted with or without the outer pressure casing, dependent on the test carried out.

The gear pump drive shaft, which in operation is coupled to the impeller, is connected to a variable speed d.c. motor, giving a controlled speed range of 0 to 1000 rpm. An integral part of the motor is a tachogenerator, the voltage output being proportional to speed, providing an excellent revolution counter.

Connected to the piston ram is a 1000 kgf rated, commercially available, two way load cell to measure the compressive forces with the ram in push mode, and tensile forces when the ram is in pull mode.

A simple pulley and potentiometer arrangement, not shown on fig 2, provided a measurement of the change in spring length.

To ensure maximum oil flow through the Moog valve during these tests, a 2.5 volt battery and polarity changeover switch provided a 10 milli-amp signal to the valve solenoids.

An additional feature of the test rig, but not used for this report, is the cycling test unit. This provides a changeover switching arrangement of the Moog valve drive signal, allowing long term cycling tests under controlled conditions. A circuit diagram of the changeover unit is shown in fig.3.

## **4.0 TESTING PROGRAMME, PROCEDURES AND RESULTS**

### **4.1 Testing Programme**

Two experiments were carried out to ascertain the performance of the hydraulic units. The first, the end plate load test, was a basic test where the free end of the load cell was attached to the bench end plate. From this arrangement, measurements could be taken, showing the relationship between impeller speed, oil pressure, input power and the maximum push and pull forces exerted by the ram.

The second test, the spring load test, were measurements taken with the free end of the load cell connected to a coiled spring. By measuring the spring compression, the forces involved in doing this work and also the input power to the drive motor, it is possible to calculate the work capability of the unit as well as its overall efficiency.

The primary difference between the End Plate tests and the Spring Load tests is that the former is a test where the unit has reached a stable state before measurements are taken, while the latter is a dynamic test where parameters are measured during the transient phase when the spring is being compressed.

### **4.2 Procedures and Results**

Before going into the main test programme it was first necessary to evaluate the power losses in the dc motor in order to derive a realistic figure for the input power of the hydraulic motor.

#### **4.2.1 Motor losses**

$$\text{HYD.UNIT I/P POWER (Watts)} = \text{MTR.I/P POWER} - \text{MTR LOSSES}$$

Motor losses can be resolved into two groups: the speed sensitive losses and the load sensitive losses.

The motor speed related losses are mainly those associated with eddy currents and hysteresis. However, the motor used in these tests was a permanent magnet type with no moving iron in its magnetic field, thus these speed related "iron losses" were near zero. With the motor off load, a series of motor current and speed measurements were taken for differing applied voltages and the results plotted in fig.4. Inspection shows an approximate current change from 0.2 Amps to 0.36 Amps over a motor speed range

from 100 rpm to 500 rpm. With a combined motor armature and brush resistance of 1.0 Ohms, the dissipation varies from 0.04 Watts to 0.13 Watts of heat which can be discounted when compared to the load related heat losses.

The load sensitive loss is the power dissipated in the motor armature resistance,  $I^2R$ , and is dependant on the torque generated in response to the load demand and hence to armature current.

$$\begin{aligned} \text{MOTOR LOSSES(Watts)} &= (\text{MTR CURRENT(Amps)})^2 \times \text{MTR. RESISTANCE(Ohms)} \\ &= (I)^2 \times 1.0 \text{ Watts.} \end{aligned}$$

Inspection of the spring load test data show that the change in motor current during spring compression is quite significant, and varies for each unit. Therefore these load sensitive losses have to be accounted for if a realistic figure for the motor power losses and hence the hydraulic input power is to be derived.

#### **4.3 End Plate Load Test**

As previously mentioned, the load cell for this test is bolted to the bench end plate. With a pressure gauge connected to the high pressure line, a series of measurements were taken on three hydraulic units over a motor speed range 30 to 300 rpm. At each speed change sufficient time was given for the system to stabilise before instrument readings were taken.

Parameters measured were:

- Motor input voltage.
- Motor input current.
- Impeller shaft speed in rpm.
- Hydraulic oil pressure.
- Load cell forces.

From these data, the power was calculated and plots produced for each unit, figs 5, 6 and 7, illustrating the relationship between pressure, force and hydraulic unit input power with impeller shaft speed.

#### **4.4 Spring Load Test**

To evaluate the power output capabilities of the hydraulic units, and hence the power required to operate the system, it is necessary to take measurements when the units are actually doing work and for this, a 305 mm spring with a maximum load rating of 9502 N was attached to the load cell. To maintain the same load conditions for all the tests, a set of change over rods enabled the spring to be kept under compressive load for both push and pull conditions of the hydraulic unit.

Using a 4 channel chart recorder, changes in spring length, load, motor speed and motor input current were plotted against time for the five units under test.

A copy of the plots for each of the five units, operated in the push mode, are shown in figs 8, to 12 inclusive, and for pull mode operation in figs 13 to fig 17 inclusive. For these tests the motor speed was kept at or near the operational speed of 150rpm.

From each of the plots of figs 8 to 17 inclusive the data were extracted for each parameter at the point where the spring was compressed by 43mm. The reason for this particular spring length was because it was found that this was the largest spring compression that was common to all the test data sets. Using this information, the input and output power and work done, was calculated to provide an assessment of the performance for each unit. The method of calculation, the extracted data and the results for unit number 1 in push mode are fully described in Section 4.5 below. A complete tabulation of the results for all of the units, in push and pull modes, is shown in table 1 and table 2. respectively.

#### 4.5 Hydraulic Unit No.1 Performance Calculations

Although the calculations are fairly basic, an explanation of some of the operations for the non engineers are included which may be of assistance for ease of understanding. Where force is a constant:

Work done = force x distance moved in the direction of the force.

However in the spring test, the force is not a constant and the work done in compressing a spring may be represented by the work diagram shown in fig. 18.

$$\text{WD} = \int_{x_0}^{x_1} F \cdot dx \quad \text{where } F = \text{applied force}$$

$x_0$  = initial compression  
 $x_1$  = final compression

but  $F = Cx$  where  $C$  = Spring Constant

$x$  = total spring compression.

$$\text{Thus WD} = \int_{x_0}^{x_1} Cx \cdot dx$$
$$= \left. \frac{1}{2} Cx^2 \right|_{x_0}^{x_1}$$

if  $x_0 = 0$

$$\text{Then WD} = \frac{1}{2} \cdot C \cdot x_1 \cdot x_1$$
$$= \frac{1}{2} \cdot F \cdot x$$

= Area of triangle abc.

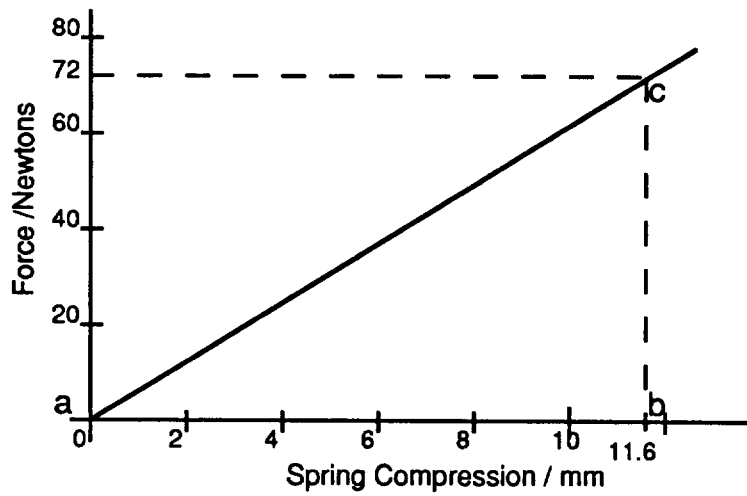


Fig. 18: Spring work diagram

$$\begin{aligned}
 \text{WORK DONE} &= 1/2 \times \text{FORCE} \times \text{CHANGE IN LENGTH} \\
 \text{Area of triangle abc} &= 1/2 \times \text{base} \times \text{height} \\
 \text{WORK DONE (Joules)} &= 1/2 \times \text{CHANGE IN LENGTH (Metres)} \times \text{FORCE (Newtons)} \\
 &= 1/2 \times (11.6/1000) \times 72 \\
 &= 0.418 \text{ Joules.}
 \end{aligned}$$

From the data in fig 18

Power is the rate of doing work.

$$\text{POWER (Watts)} = \text{WORK DONE (Joules)} / \text{TIME(Seconds)}$$

But for the motor:

$$\text{MTR.I/P POWER (Watts)} = \text{AVERAGE CURRENT (Amps)} \times \text{VOLTAGE (Volts)}$$

$$\begin{aligned}
 \text{HYD.UNIT I/P POWER (Watts)} &= \text{MTR.O/P POWER (Watts)} \\
 &= \text{MTR. I/P POWER} - \text{MTR. LOSSES}
 \end{aligned}$$

$$\begin{aligned}
 \text{MOTOR LOSSES(Watts)} &= (\text{MTR CURRENT(Amps)})^2 \times \text{MTR.RESISTANCE(Ohms)} \\
 &= (I)^2 \times 1.0 \text{ Watts}
 \end{aligned}$$

IOS HYDRAULIC UNIT No. 1 (Test data extracted from fig 8.)

PUSH MODE.

SPEED	= 180 rpm
LOAD START	= 120 kgf
LOAD END	= 710 kgf
CHANGE IN LOAD	= 590kgf
	= 590 x 9.81 Newtons
	= 5788 Newtons
SPRING COMPRESSION	= 43 mm
MOTOR CURRENT START (I <sub>1</sub> )	= 1.8 Amps
MOTOR CURRENT END (I <sub>2</sub> )	= 4.5Amps
CHANGE IN CURRENT	= 2.7 Amps
MOTOR VOLTAGE	= 15 Volts
TIME TAKEN (t <sub>2</sub> )	= 13.2 Secs.
WORK DONE (Joules)	= FORCE (Newtons) x DISTANCE (Metres)
	= (1177 x 0.043) +(5788 x 0.5 x 0.043)
	= 50.6 + 124 Joules
	= 174.6 Joules
OUTPUT POWER(Watts)	= WORK DONE (Joules) / TIME (Secs)
	= 174.6/13.2
	= 13.2 Watts
TOTAL MOTOR INPUT POWER(Watts)	= AVERAGE CURRENT (Amps) x VOLTS
	= ( 1.8 x 15 ) + ((2.7/2) x 15 )
	= 47.25 Watts
MOTOR LOSSES (Watts)	= (AV. CURRENT(Amps)) <sup>2</sup> x MTR. RES.(Ohms)
	= $\frac{1}{t_2} \int_{t_1}^{t_2} I^2 \cdot R \cdot dt$ where R = 1.0 Ohm



which simplifies to 
$$= \frac{(I_2^3 - I_1^3)}{3(I_2 - I_1)}$$

$$= 10.53 \text{ Watts}$$

HYD. UNIT I/P WORK (Joules) 
$$= \text{POWER} \times \text{TIME}$$

$$= (47.25 - 10.53) \times 13.2$$

$$= 485 \text{ Joules}$$

POWER EFFICIENCY (%) 
$$= (\text{POWER OUTPUT} / \text{POWER INPUT}) \times 100$$

$$= (13.26 / (47.25 - 10.53)) \times 100$$

$$= 36 \%$$

**Table 1**

**PUSH MODE.**

**Spring Test Data**

		1	2	3	4	5	
	UNITS	Fig. 8.	Fig. 9.	Fig.10.	Fig.11.	Fig.12.	MEAN
MOTOR SPEED.	rpm	180	160	180	190	170	176
LOAD START	kgf	120	120	120	120	120	120
LOAD END	kgf	710	720	660	660	700	690
LOAD CHANGE	Newtons	5788	5886	5297.	5297.	5690	5592
SPRING EXTENSION	mm	43	43	43	43	43	43
MTR. CURRENT START	Amps	1.8	1.7	1.9	1.25	1.6	1.65
MTR. CURRENT END	Amps	4.5	5	4.85	3.8	4.95	4.62
CURRENT CHANGE	Amps	2.7	3.3	2.95	2.55	3.35	2.97
TIME TAKEN	Secs.	13.2	16.5	13.2	11.4	13.4	13.54
MOTOR VOLTAGE	Volts	15	15	15	15	15	15
O/P WORK DONE	Joules	175	177.1	164.6	165	172.9	171
HYD.UNIT O/P POWER	Watts	13.26	10.73	12.5	14.4	12.9	12.8
MTR. I/P POWER.	Watts	47.25	50.25	50.6	37.9	49.125	47
MTR. LOSSES.	Watts	10.53	12.13	12.11	6.92	11.7	10.7
HYD.UNIT I/P POWER	Watts	36.72	38.12	38.5	31	37.4	36.4
HYD. UNIT I/P WORK	Joules	485	629	508	353	501	495
POWER EFFICIENCY.	%	36	32	32.5	46	34.5	36.2

**Table 2**

**PULL MODE.**

**Spring Test Data**

	UNITS	1	2	3	4	5	
		Fig.13.	Fig.14.	Fig.15.	Fig.16.	Fig.17.	MEAN
MOTOR SPEED	rpm	165	130	175	190	165	165
LOAD START	kgf	0	0	0	0	0	0
LOAD END	kgf	520	550	520	560	520	534
LOAD CHANGE	Newtons	5101	5395	5101.	5493	5101.	5239
SPRING EXTENSION	mm	43	43	43	43	43	43
MTR.CURRENT START	Amps	1.3	1.5	1.2	1.1	1.7	1.36
MTR. CURRENT END	Amps	5.3	7.9	5.5	4.95	5.3	5.79
CURRENT CHANGE	Amps	4	6.4	4.3	3.85	3.6	4.43
TIME TAKEN	Secs.	9.6	9.6	13	9	10	10.24
MOTOR VOLTAGE	Volts	15	15	15	15	15	15
O/P WORK DONE	Joules	109.7	116	109.7	118.2	109.7	112.6
HYD.UNIT O/P POWER	Watts	11.42	12.08	8.44	13.13	10.96	11
MTR. I/P POWER	Watts	49.5	70.5	50.25	45.4	52.5	53.6
MTR. LOSSES	Watts	12.22	25.5	12.8	10.4	13.33	14.9
HYD.UNIT I/P POWER	Watts	37.28	45	37.5	35	39.17	38.8
HYD. UNIT I/P WORK	Joules	358	432	487	315	392	397
POWER EFFICIENCY	%	30.6	27	22.5	37.5	28	29

In order to give a general indication of the expected performance of a typical hydraulic unit, we have averaged the data from all the units in table 1 and table 2 and presented these averages in the final column of the respective table.

## 5.0 ANALYSIS

### 5.1 Push and Pull Force Differences

Inspection of the End plate test plots, figs. 5, 6 and 7, highlight the differences in the forces measured in the push and pull modes. This can be attributed to the differences in the active areas of the piston.

From the engineering drawings, the effective piston area in push mode is 1338 mm<sup>2</sup> while in the pull mode this is reduced by the ram area to 950 mm<sup>2</sup>. From the relationship:

$$\text{FORCE} = \text{PRESSURE} \times \text{AREA}$$

the forces generated in push and pull modes are related to the piston areas, given the same pressure. It would be expected therefore that using the engineering drawing measurements, the pull forces would be reduced by the ratio of the pull to push piston areas. In this case:

$$950/1338 = 0.71$$

From figs. 5, 6 & 7, the test data plots for units 1, 2 & 3 respectively, these area ratios were calculated and compared with the engineering design value of 0.71. The information is shown in table 3 and comparison indicates that the discrepancy from 0.71 could be accounted for by wear and experimental errors.

**Table 3**

**End plate test data**

UNIT.	PRESS.	Push FORCE	Pull FORCE	Push AREA	Pull AREA	Area RATIO
	kN/m <sup>2</sup>	N	N	mm <sup>2</sup>	mm <sup>2</sup>	
1	6378	9110	5688	1428	892	0.63
2	6205	8267	5462	1332	880	0.66
3	5929	7581	5492	1278	926	0.72

From the spring test data tables, inspection of the averaged data suggests a difference in the work done to compress the spring in the push and pull modes, although the work done should be identical, as the spring compression was 43mm in each case. From tables 1 and 2:

$$\text{Pushing load change} = 5592\text{N} \text{---(1)}$$

$$\text{Pulling load change} = 5239\text{N} \text{---(2)}$$

$$\text{Difference} = 353 \text{ N} \text{---(3)}$$

$$\text{Spring constant, (SC) (N/mm)} = \text{Force(Newtons)/Compression (mm)}$$

$$\text{From (1) Pushing} \quad \text{SC} = 5592/43$$

$$= 130 \text{ N/mm}$$

$$\text{From (2) Pulling} \quad \text{SC} = 5239/43$$

$$= 122 \text{ N/mm}$$

$$\text{Mean SC} = 126 \text{ N/mm}$$

From (3), the equivalent spring length error

$$= 353/126$$

$$= 2.8\text{mm.}$$

One source of error was eventually found to be the spring mounting plate which, under full compression and tensile load conditions, exhibited a deflection difference of 1.9 mm. The manufacturers catalogue figure of 124N/mm for the spring constant, compares favourable with the 126N/mm obtained from these tests.

## 5.2 Power Losses

In an attempt to resolve and identify some of the power losses within the hydraulic system, it is necessary to utilise the data obtained from both tests.

A study of the End Plate test data shows that when the oil pressure has reached the relief valve pressure (approximately 850 psi), power continues to increase as the impeller revolutions increase. The pump pressure is fairly constant and the force plots also indicate that the load on the pump by the Moog valve and piston assembly is also little changed. This continuing increase in power loss can therefore be attributed to operating the relief valve spring and in heating up the oil. In operation, the wing is always moving and it is doubtful that the relief valve is opened for any length of time, however for any long term bench test this could result in overheating.

Inspection of the Spring Load test plots can provide a guide of the power losses that can be expected in the impeller shaft and pump. At the instant when the Pull test is initiated, by reversing the oil flow in the Moog valve, the average motor current is approximately 1.36 Amps, the pressure in the system is collapsing, and the differential pressure across the pump near zero. If this is correct, then the work done by the pump is zero and the loading on the pump is near zero which suggests that the input power is being dissipated as heat in the shaft seals and the gears in the pump.

$$\text{MOTOR INPUT CURRENT} = 1.36 \text{ Amps}$$

$$\text{MOTOR INPUT POWER} = (1.36 \times 15) \text{ Watts}$$

$$= 20.4 \text{ Watts}$$

$$\text{MOTOR LOSSES} = (1.36)^2 \times 1.0 \text{ Watts}$$

$$= 1.85 \text{ Watts}$$

$$\text{FRICTIONAL LOSSES} = 20.4 - 1.85$$

$$= 18.55 \text{ Watts.}$$

From the average results shown in table 2 further losses of 9.25 Watts ( 38.8 -11 -18.55) occur in the Pull mode when the spring is being compressed through 43mm. The pressure during this period does not reach the relief valve operating level so losses cannot be attributed to this area but are probably due to leakages in the Moog valve and frictional forces in the shaft through the end plate.

The End Plate plots also highlight the differing power demand from each unit: for example, at 150 rpm, unit 2 requires 65 Watts whilst units 1 & 3 only demand 50 Watts. In this instance the increase in power for unit 2 can be explained by the tighter tolerances of the pressure pump which produces relief valve pressure at 60 rpm as opposed to the other two units which only achieve this pressure at 100rpm.

### 5.3 Input and Output Torque Calculations

In any future study on alternative methods of wing control, it will be useful to have information on the input and output torque characteristics of the existing system and included here are torque calculations using the end plate test data for unit number one and dimensional information from the engineering drawings.

The diagram of fig 19, although not to scale, includes the major dimensions and illustrates the linkage arrangement between the hydraulic ram and the wing. The range of movement of the ram is 60mm which, with the wing link bar acting on a radius of 114.3mm provides a 30 degree wing angle movement.

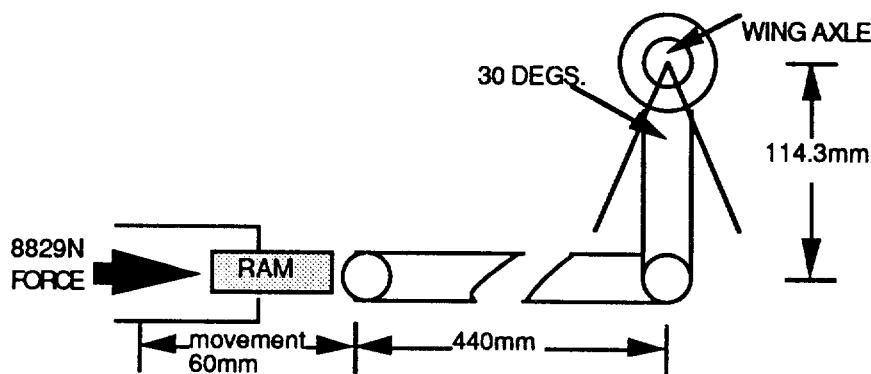


**Fig.19 Ram to wing linkage.**

Using the End Plate test plot of fig.5 for unit no.1, the ram force generated in the push mode at 150 rpm (2.5 rps) is approximately 8826N (900kgf x 9.81).

For the wing,

$$\begin{aligned} \text{PEAK O/P TORQUE (Nm)} &= \text{FORCE (N) x RADIUS (m)} \\ &= 8826 \times 0.1143 \\ &= 1009 \text{ Nm.} \end{aligned}$$

For the impeller,

$$\begin{aligned} \text{I/P TORQUE (Nm)} &= \text{POWER (W) } / (2 \times \Pi \times n(\text{revs per sec.})) \\ &= (49) / (2 \times \Pi \times 2.5) \\ &= 49 / 15.7 \\ &= 3.12 \text{ Nm.} \\ \text{TORQUE GAIN} &= 1009/3.12 \\ &= 323 \end{aligned}$$

Possible future developments could include an electrically operated system for wing control, and the power information given in tables 1 and 2 show that it is feasible. Certainly the removal of the oil and possible leaks make it an attractive proposition. However, to make this changeover an important consideration, other advantages, such as a reduction in size must be established, as a solution to the leakage problem may have already been achieved, see 5.4. Study of the torque equations above show that a 323:1 step up in torque from motor to wing is required which, if it is to be achieved using a mechanical gear box will be somewhat larger than the existing hydraulic piston and cylinder arrangement. However there are periods during the undulating cycle when the response of the vehicle is slow, particularly on turnover near the surface, and the assistance of an electric motor at these times could be advantageous.

#### **5.4 Oil Leakage Problems**

From time to time during operational deployments, problems of sea-water contamination of the hydraulic system have arisen, resulting in premature vehicle recovery and loss of data. Two leakage paths are required for sea-water to contaminate the system. The first, through the housing assembly, which includes the bellows and pressure balancing tubes, into the oil surrounding the hydraulics and, secondly,



from this outer chamber into the oilways of the hydraulic circuit itself. Past experience has shown that the most likely source of the problem is a failure of the sealing between the ram and bellows assembly. This was confirmed during these tests with an oil leakage at or near this point.

After further study of this problem, it was decided to modify one of our units by removing the bellows assembly and replacing it with an end plate to seal the four oilways and provide an extra shaft seal . Although exposed to sea-water, the chrome hardened steel ram should remain corrosion free and the shaft seals should continue to function satisfactorily. Further laboratory tests and sea trials are required before this modification can be shown to be a solution to the problem.

## **6.0 Conclusions**

It is hoped that the information provided in this document has gone some way in extending our knowledge of the SeaSoar hydraulic unit and thus satisfy the primary aim of this report.

## **7.0 Acknowledgements**

The authors wish to thank all those who contributed to this report, particularly the workshop staff who provided their expertise.

## **APPENDIX A**

### **SEASOAR HYDRAULIC UNITS**

#### **PREPARATION PROCEDURES**

1. Drain oil.
2. Inspect oil for salt water contamination
3. Strip down and inspect internal bellows for sign of leakage.
4. Install in test rig, without case.
5. Check on maximum extension of the ram that the bellows is not totally collapsed. ie indication of leak.
6. Renew oil completely if there is sign of leakage. Clean filters.
7. Connect pressure gauge (1500psi)(1035kPa.) to top of high pressure filter.
8. Bleed the system.
9. Run the motor up to 150 rpm and bleed system from the low pressure filter cap. Top up bellows with oil using syringe connected to the Schraeder valve on the reservoir bellows. Using the valve reversing test switch, continue to bleed the system to remove air. Jerky, spongy movements with the ram indicate the presence of air. The bellows should move slightly from max. to min. piston position.
10. Check and set relief valve for 900 psi (6206kPa)
11. Disconnect gauge, refit filter cap, rerun system to check for air. Bleed and top up as necessary, over 20 cycles at least.
12. Give a 24 hour time test for system to stabilise and check for leaks.
13. Refit outer casing and top up with oil. Run system to check for leakage
14. Repeat as in 12.
15. Return unit to transit case.

## **APPENDIX B**

### **Abbreviations used in this report.**

IOSDL	Institute of Oceanographic Sciences Deacon Laboratory.
m.m.	Millimetres
rpm	Revolutions per minute.
rps	Revolutions per second.
Fig.	Figure.
HP	High Pressure.
LP	Low Pressure.
kgf	Kilograms force.
N.	Newtons.
d.c.	Direct Current.
Hyd.	Hydraulic.
MTR	Motor
KN/m <sup>2</sup>	Kilo Newtons per square metre.
AV	Average.
SC	Spring Constant.
psi	Pounds per square inch

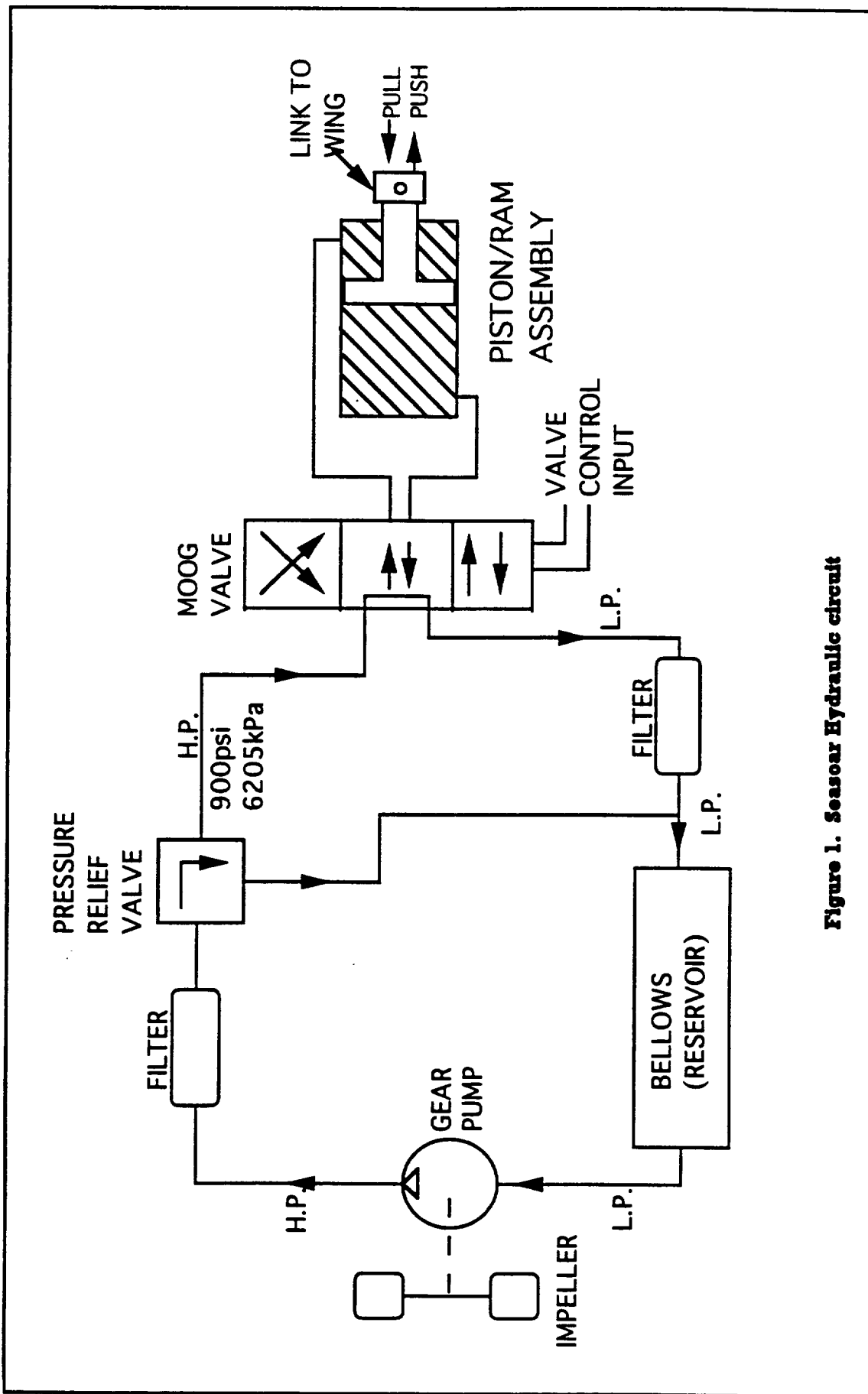
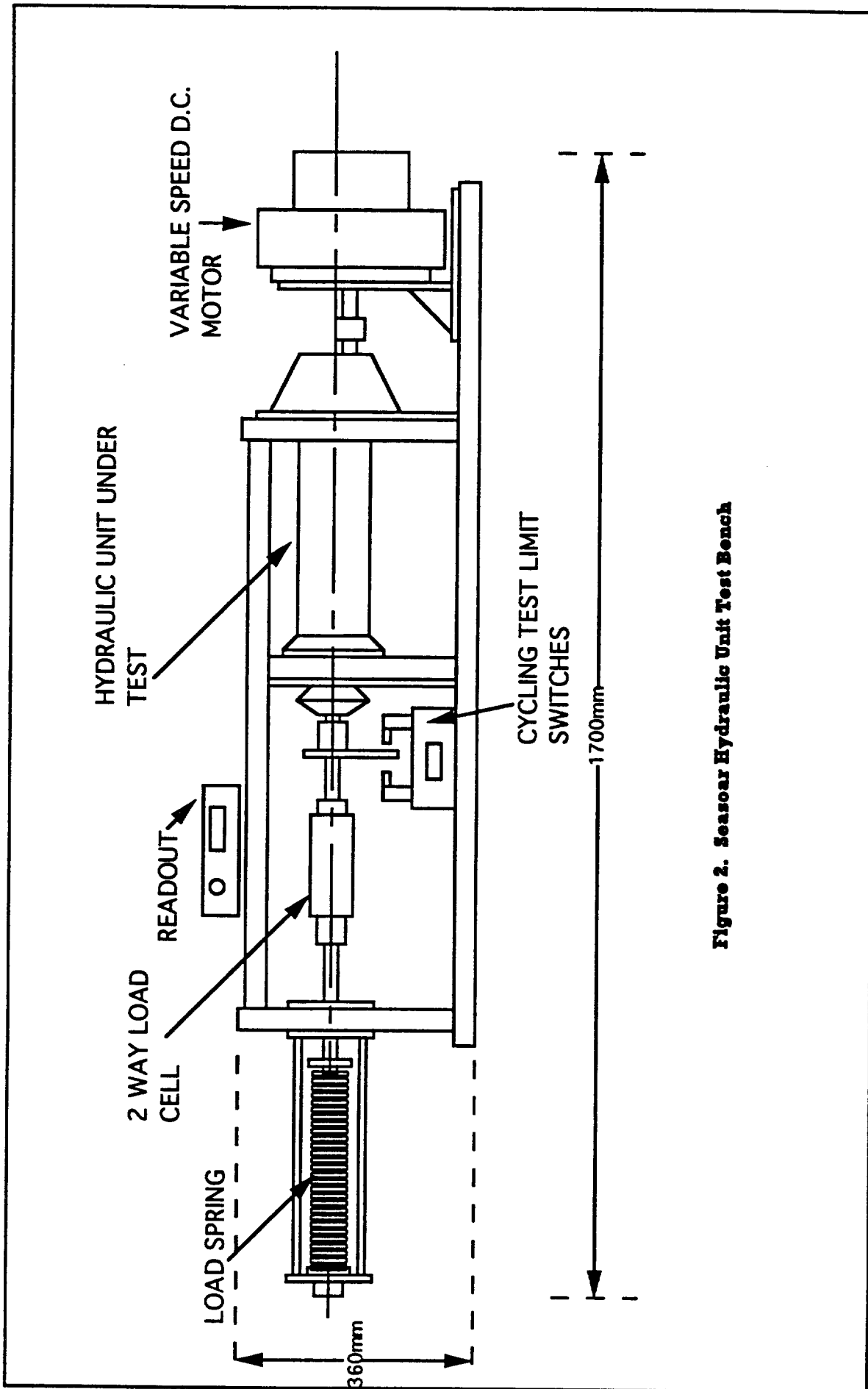


Figure 1. Seasoar Hydraulic circuit



**Figure 2. Seasoar Hydraulic Unit Test Bench**

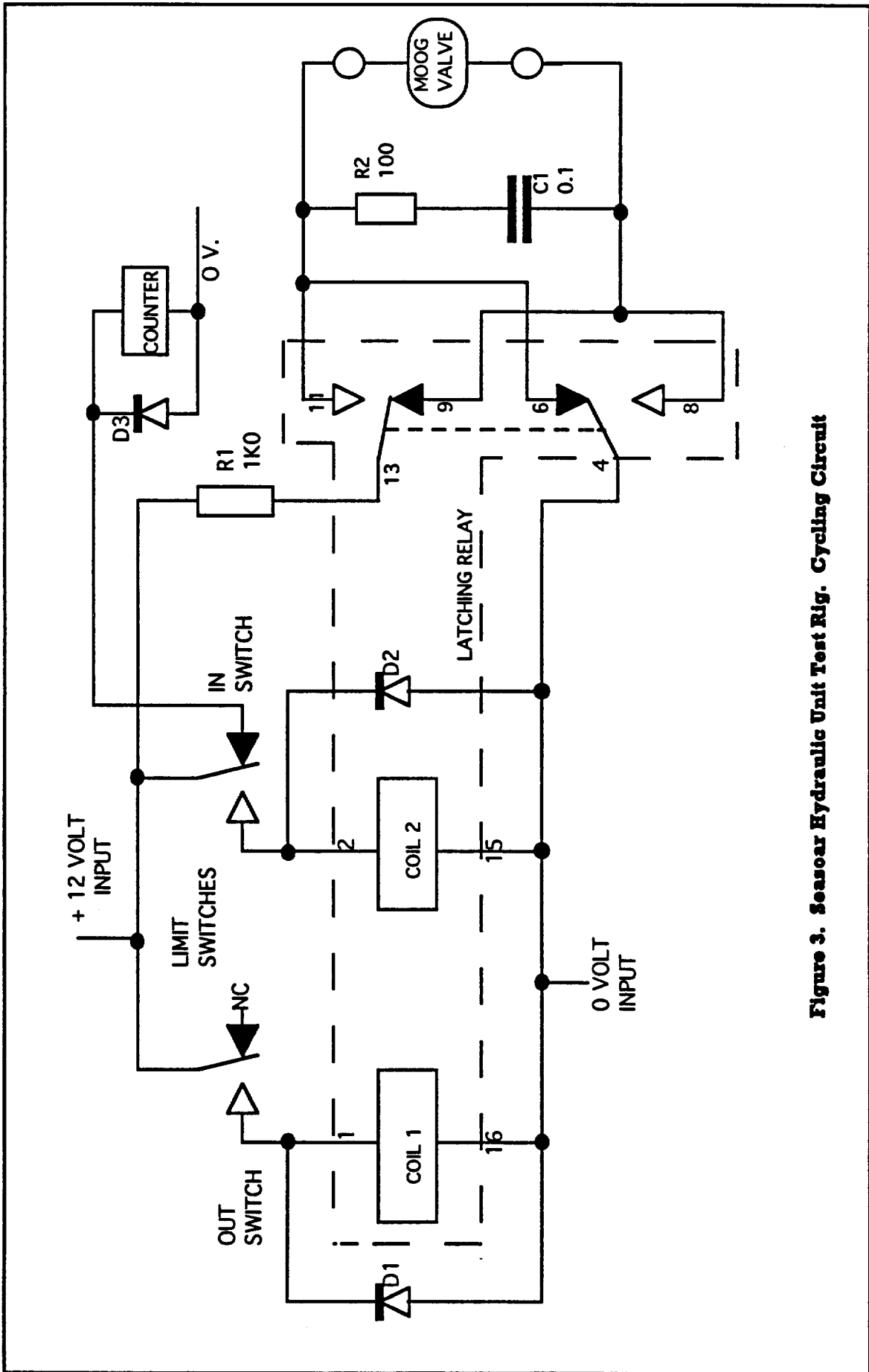


Figure 3. Seasoar Hydraulic Unit Test Rig. Cycling Circuit

# HYDRAULIC UNIT TEST RIG.

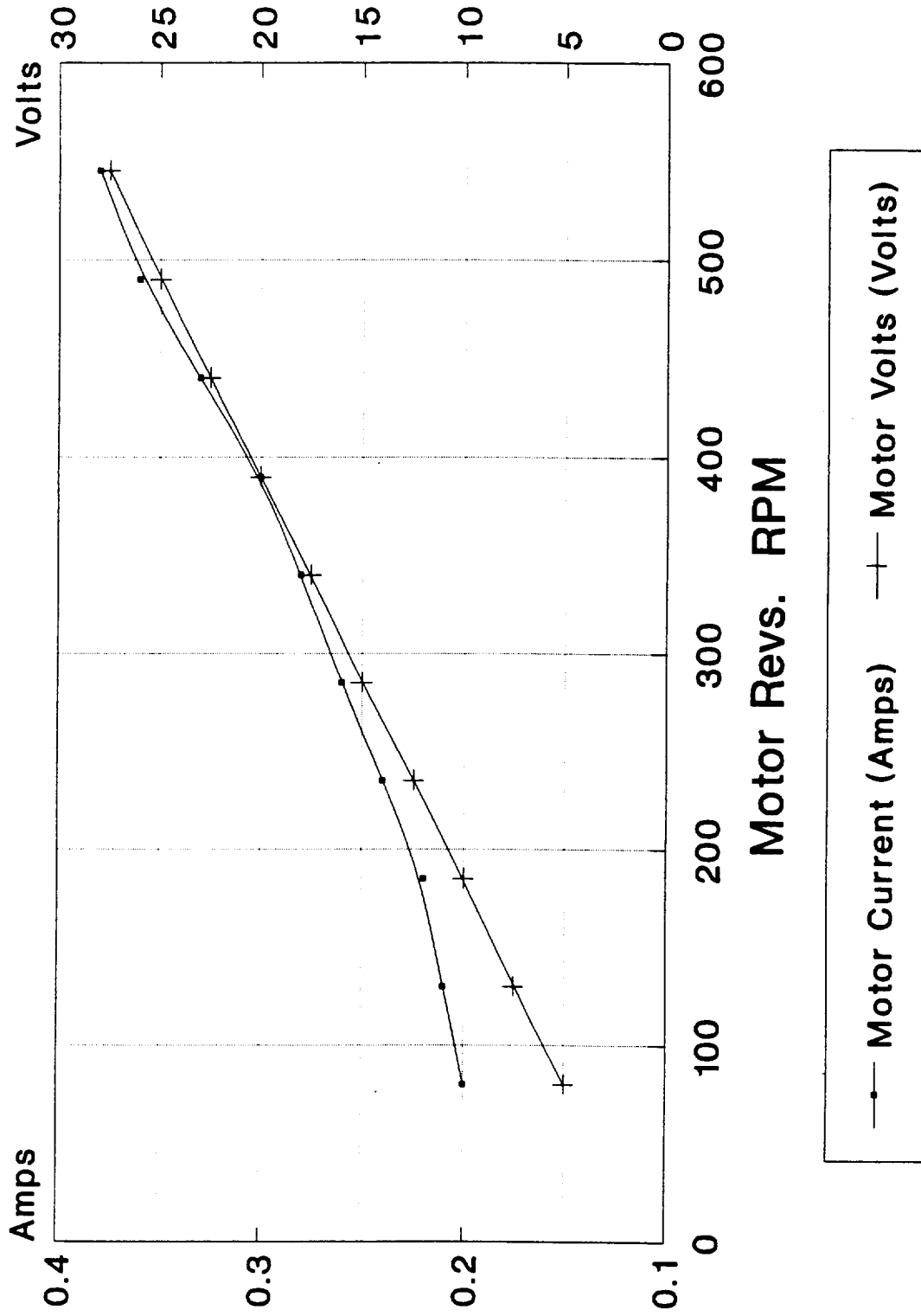


Figure 4. D.C. Motor Off load Speed Related Losses

# SEASOAR HYDRAULIC TESTS

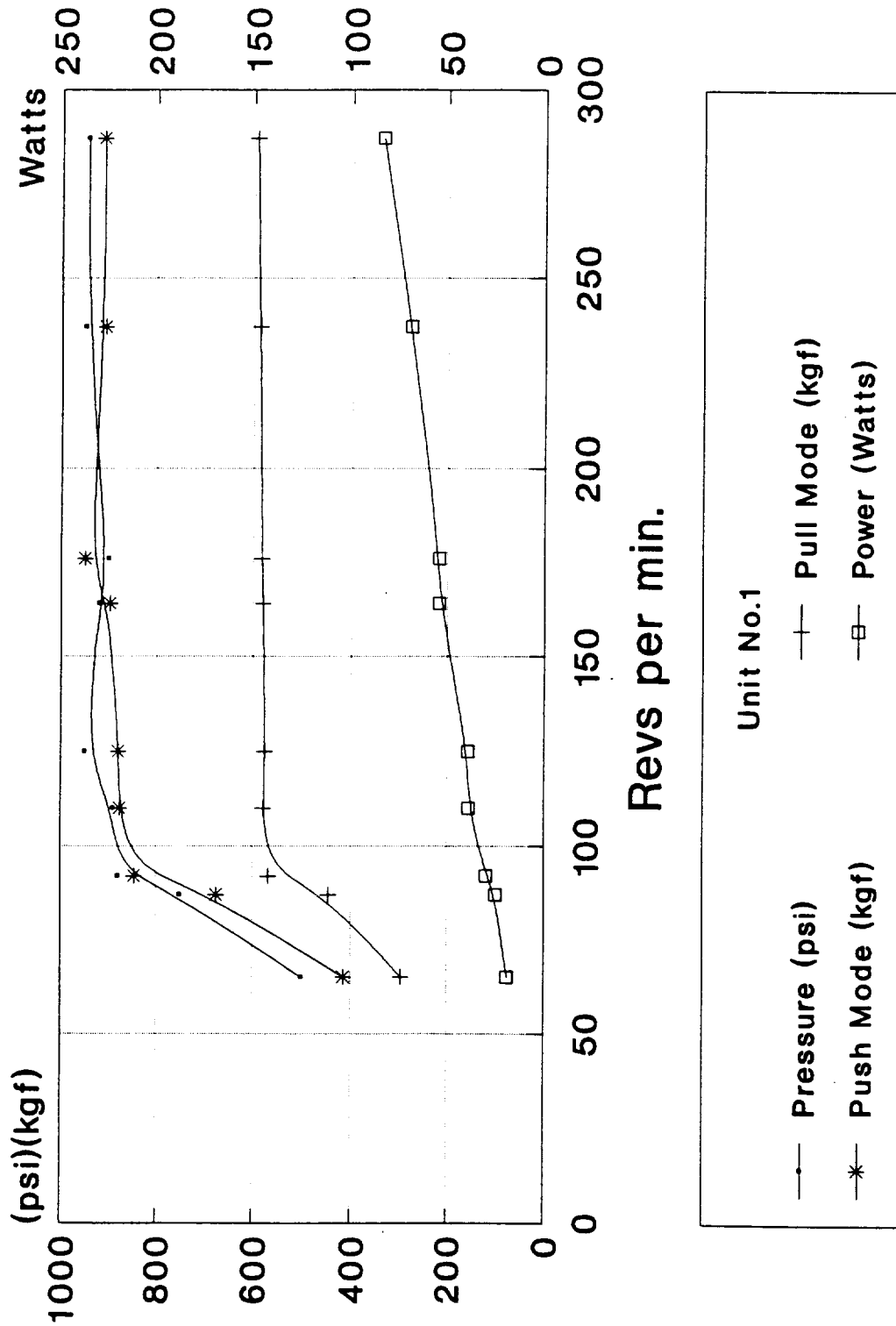


Figure 5. Unit No. 1. End Plate Tests



# SEASOAR HYDRAULIC TESTS

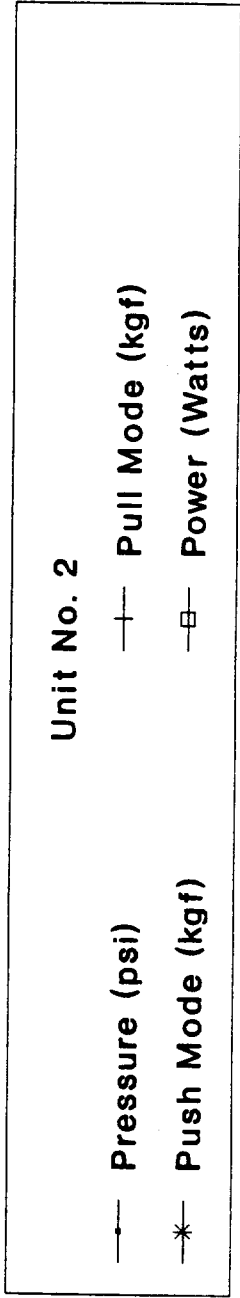
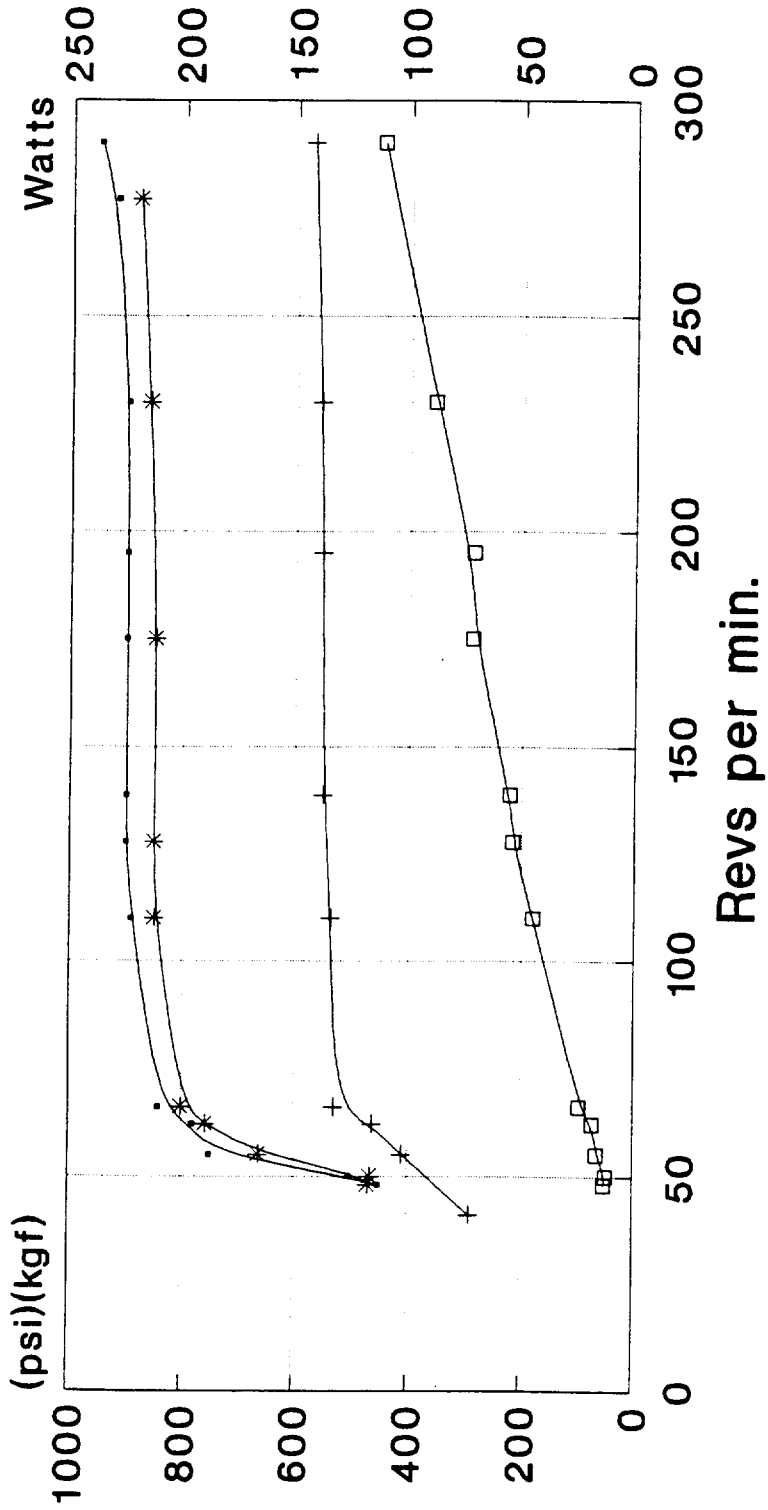


Figure 6. Unit No. 2. End Plate Tests

# SEASOAR HYDRAULIC TESTS

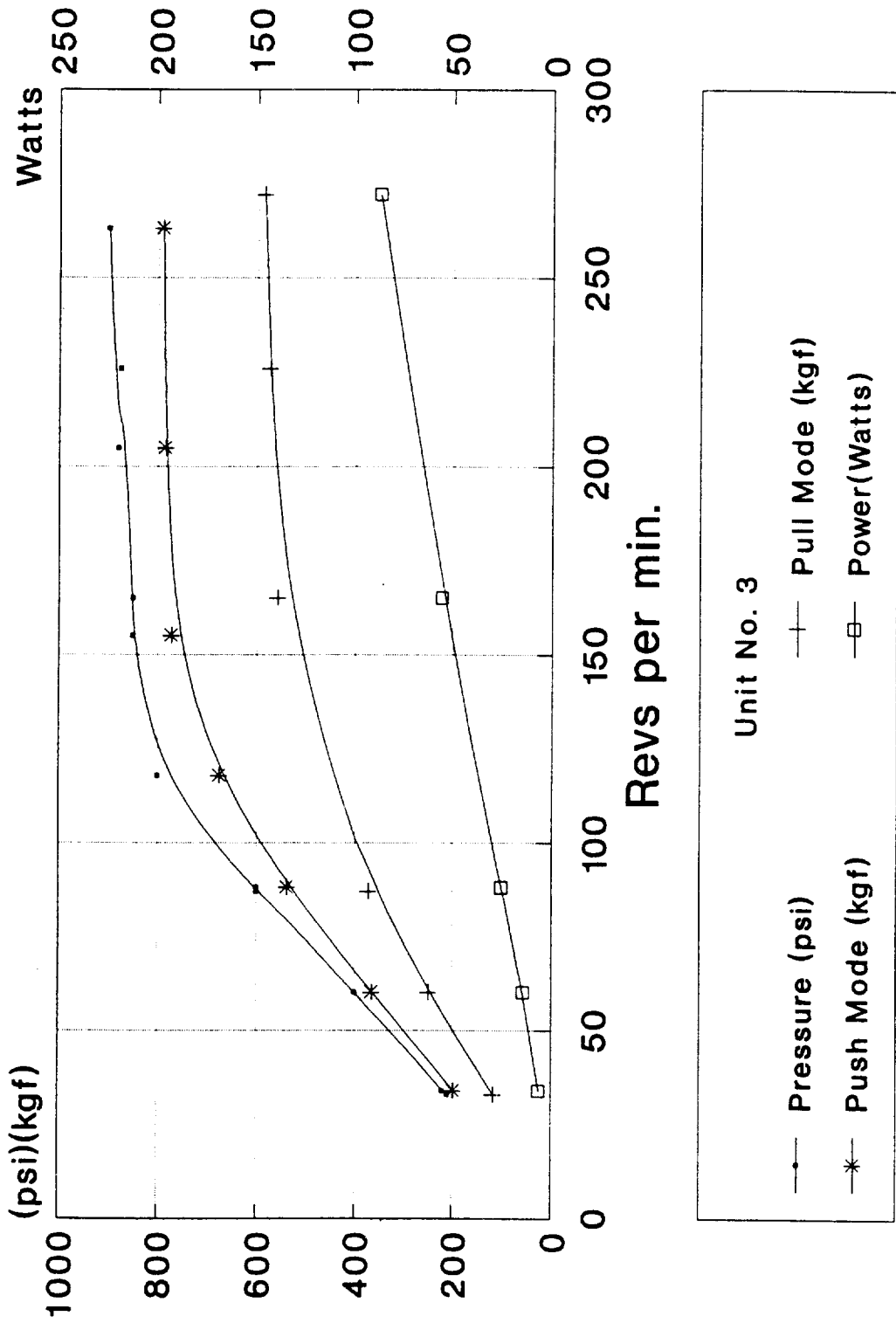


Figure 7. Unit No. 3. End Plate Tests

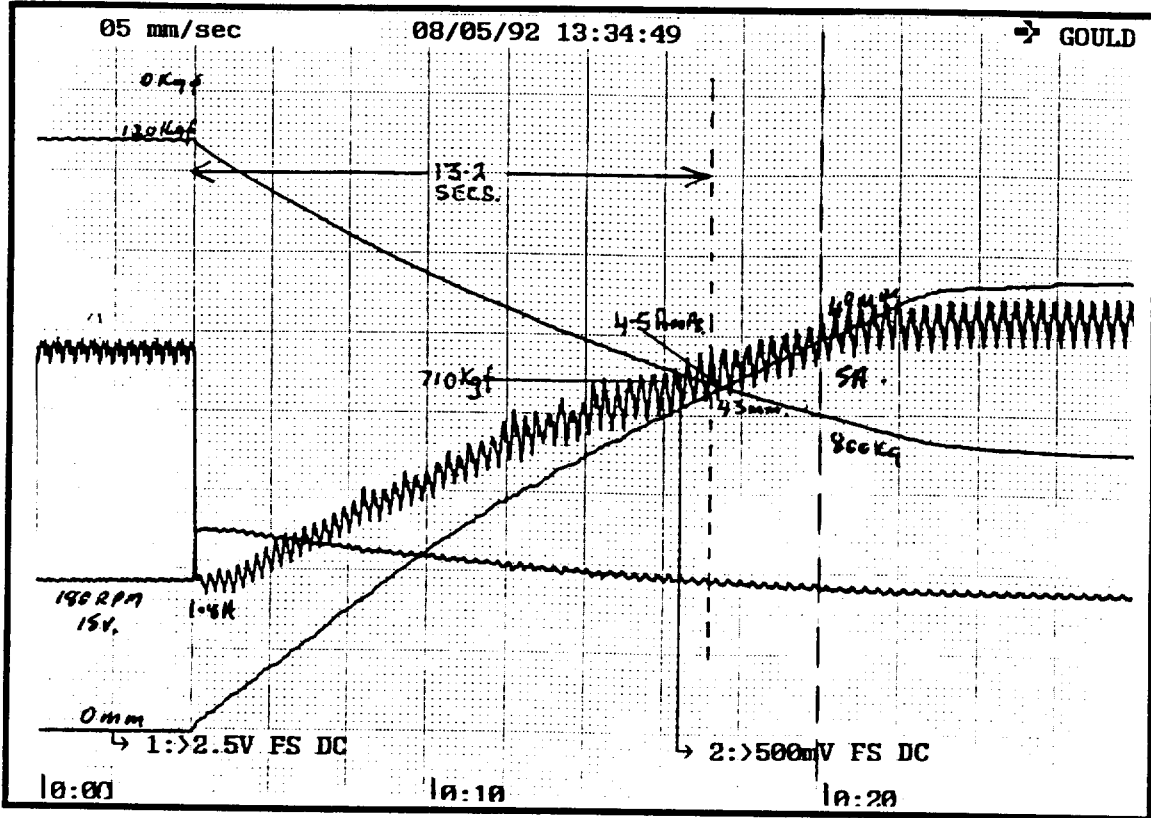


Figure 8. Unit No. 1 Push Mode

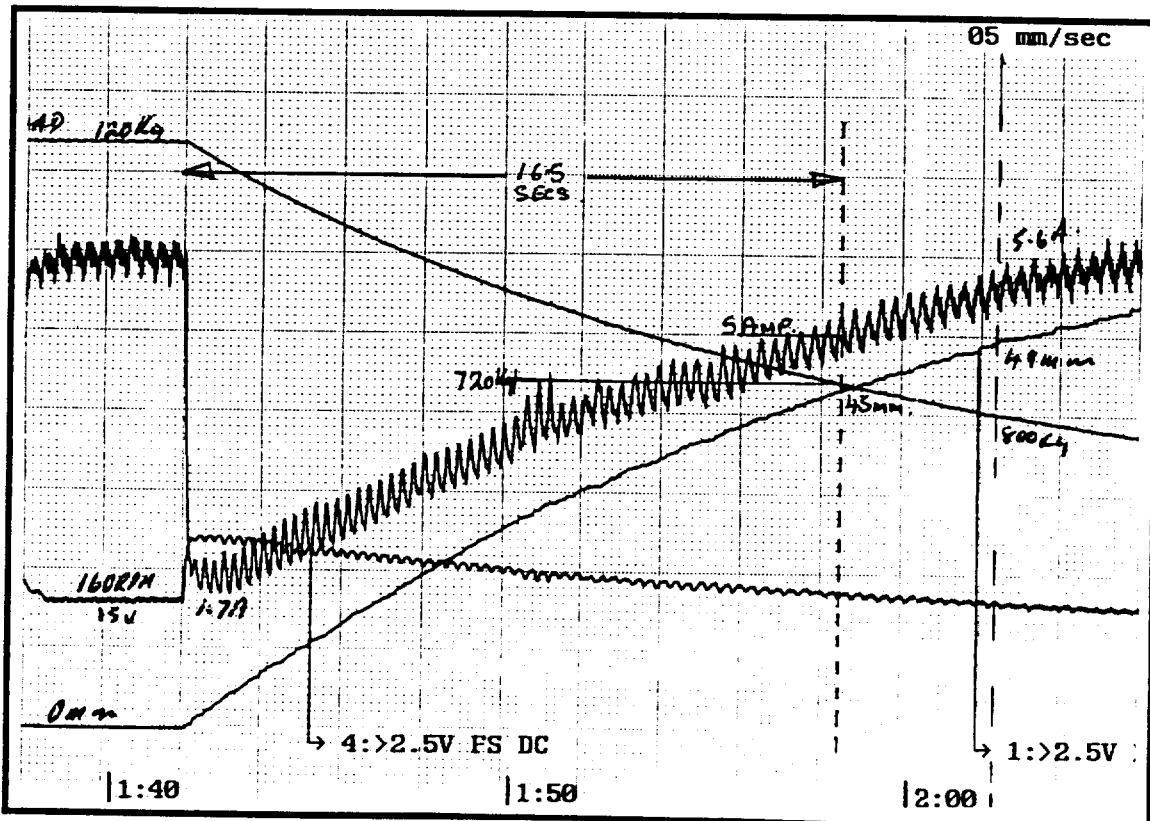


Figure 9. Unit No. 2 Push Mode

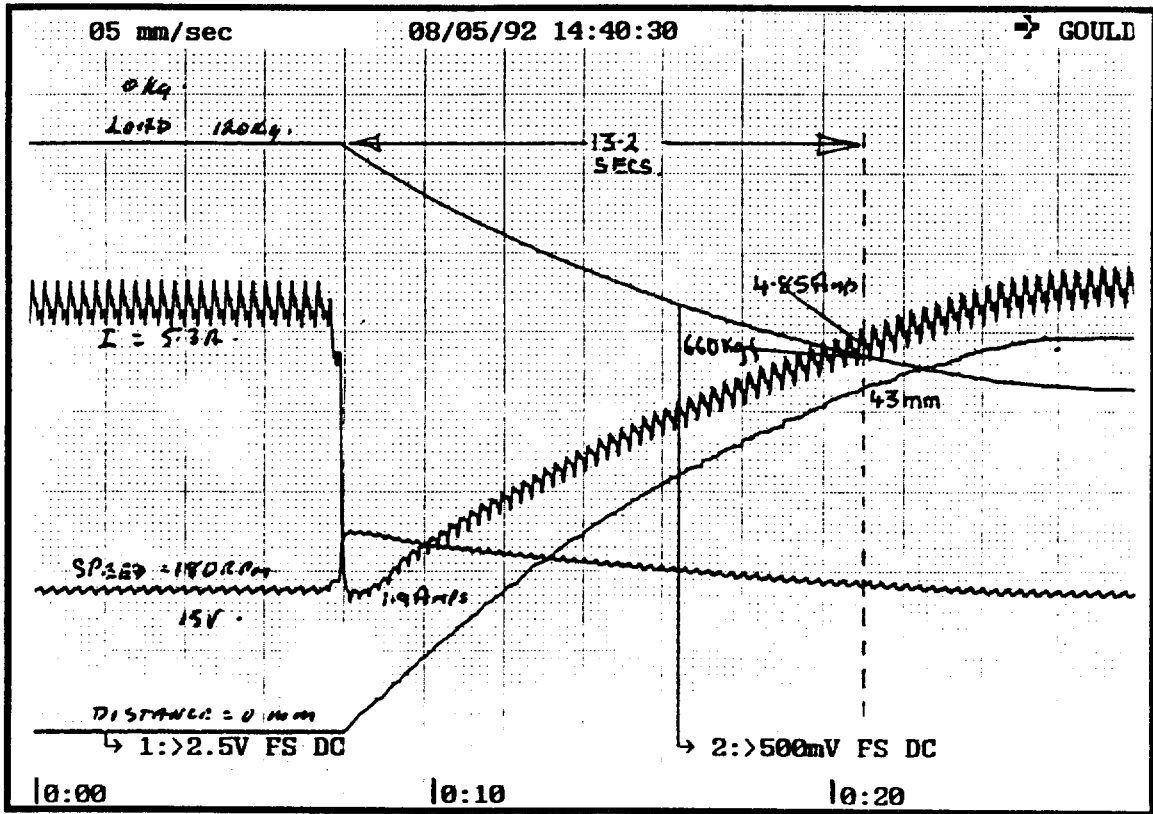


Figure 10. Unit No. 3 Push Mode

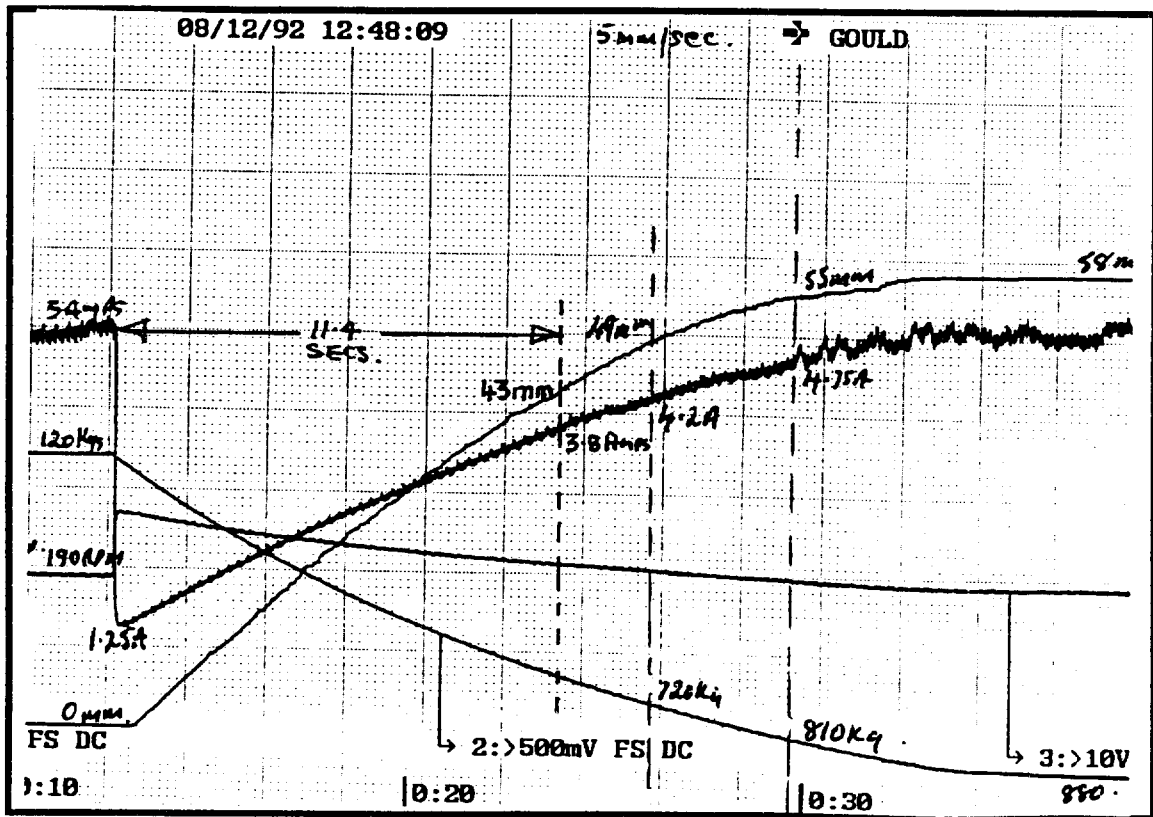


Figure 11. Unit No. 4 Push Mode

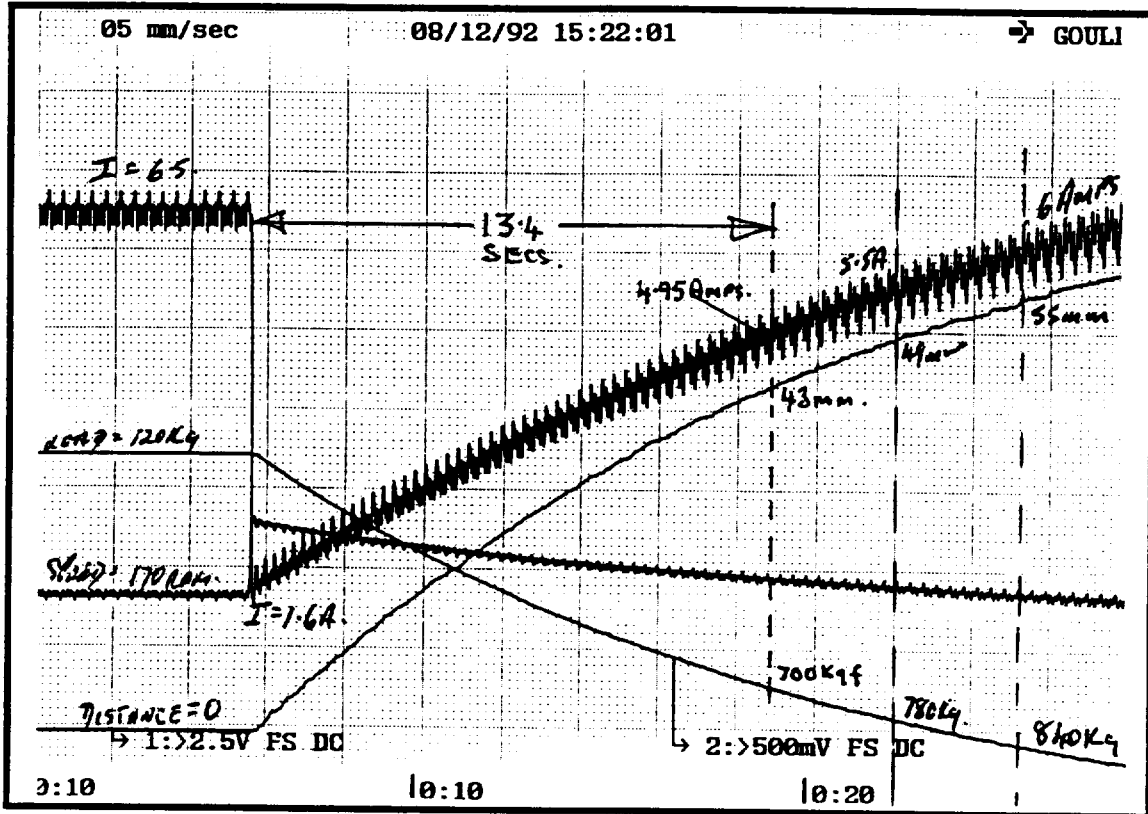


Figure 12. Unit No. 5 Push Mode

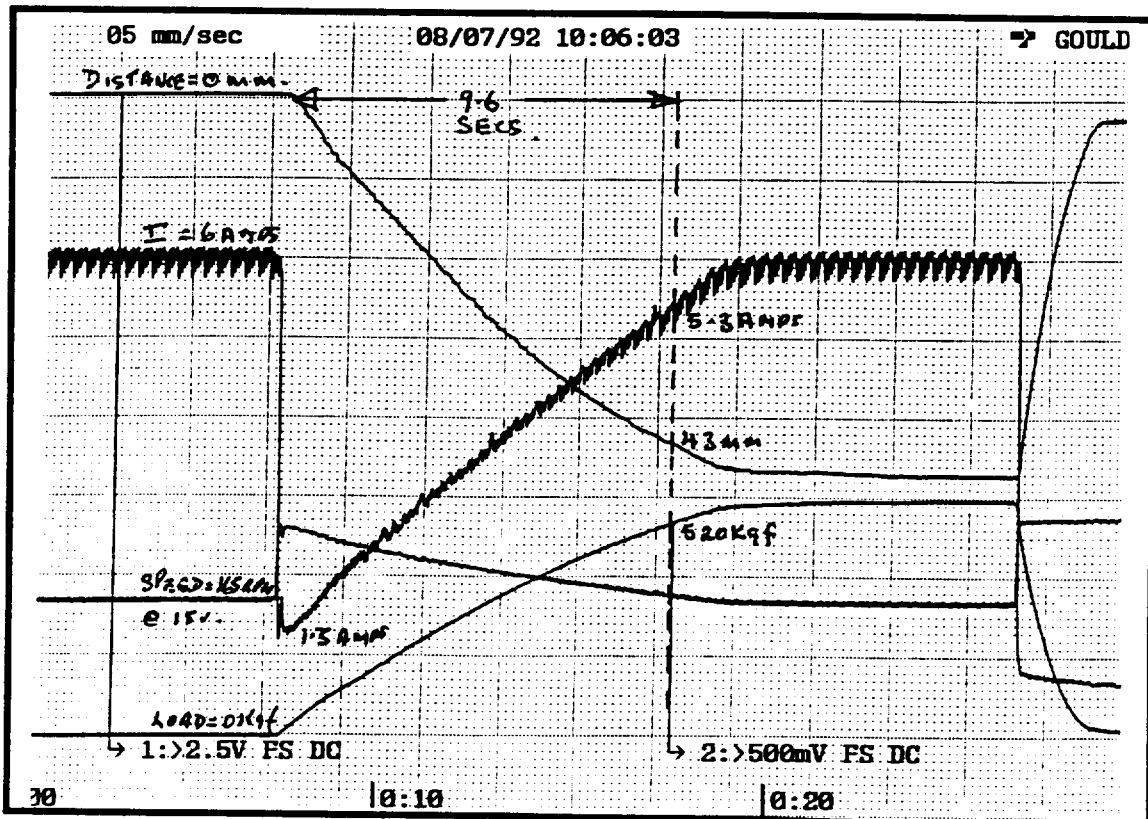


Figure 13. Unit No. 1 Pull Mode

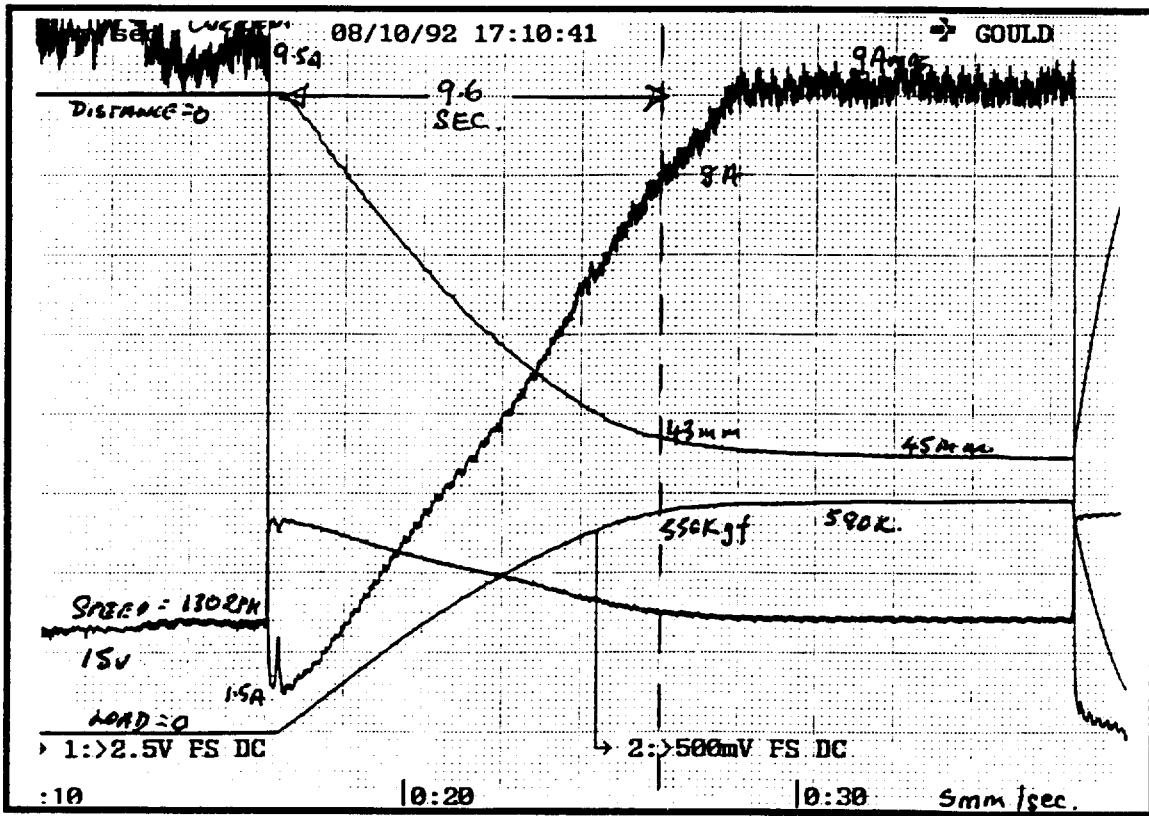


Figure 14. Unit No. 2 Pull Mode

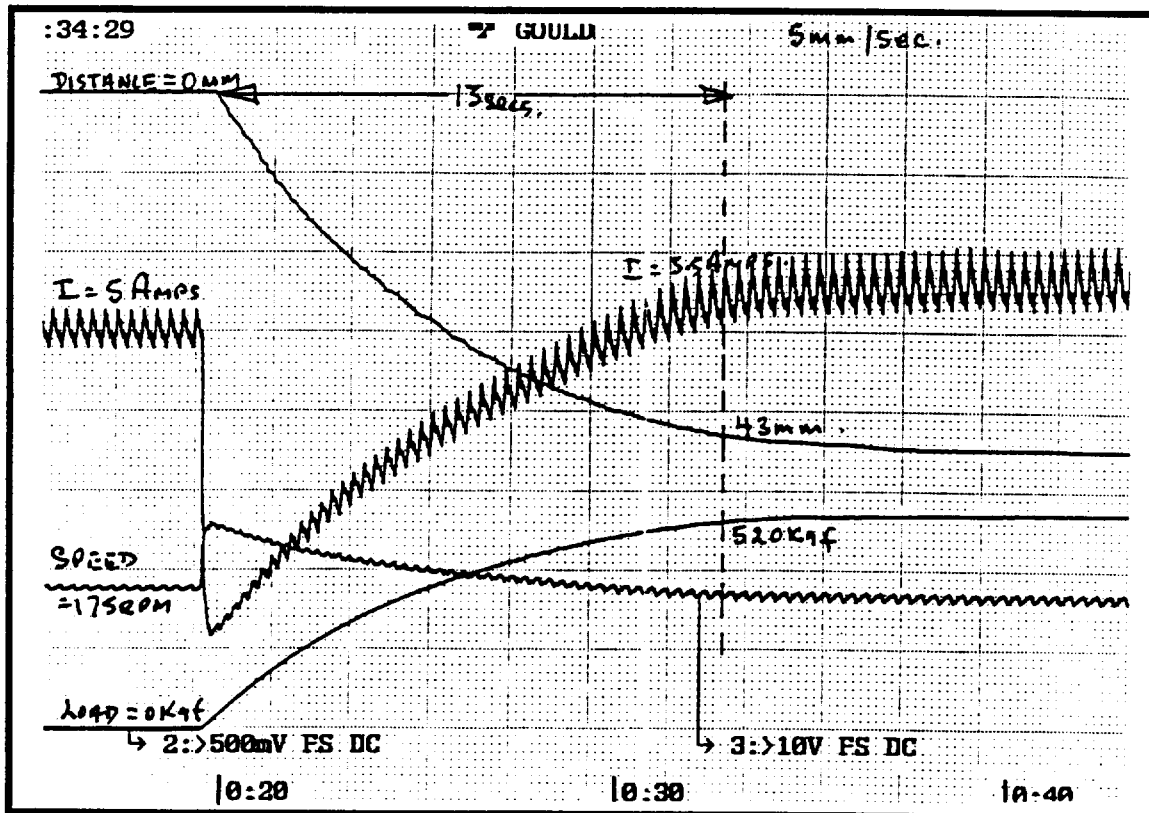


Figure 15. Unit No. 3 Pull Mode

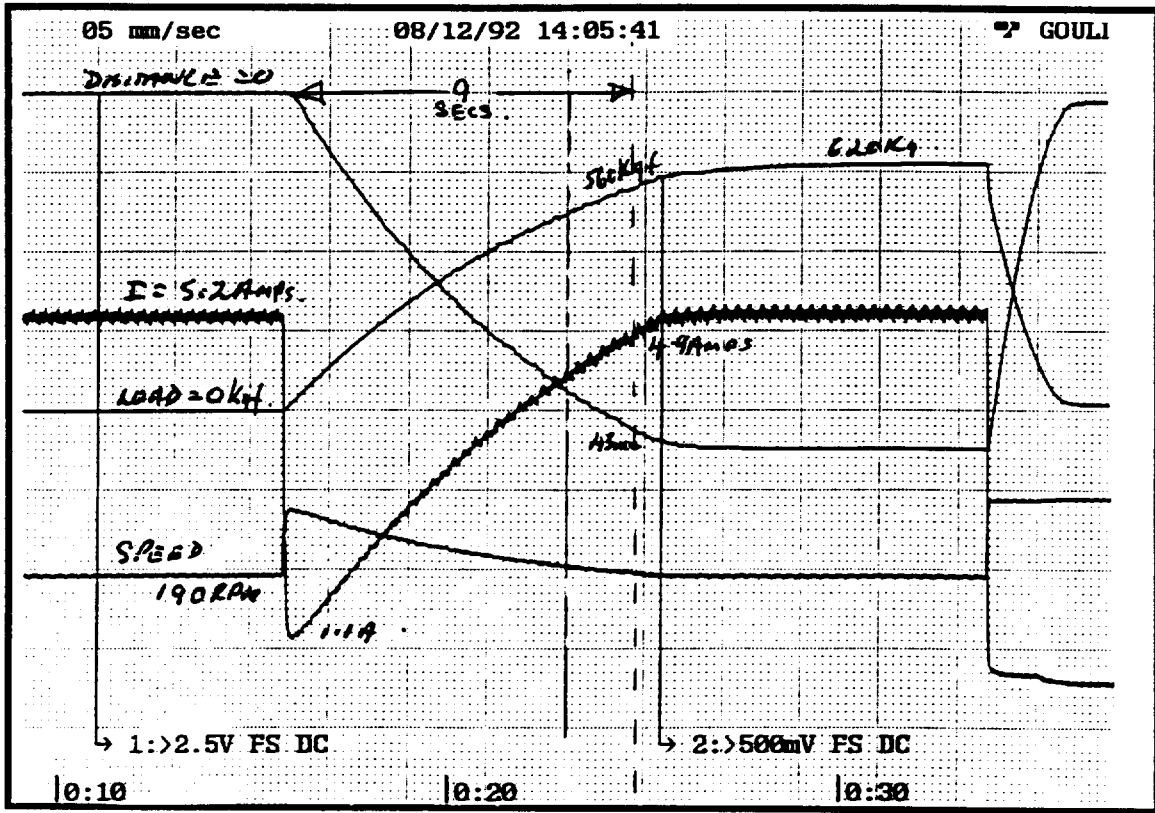


Figure 16. Unit No. 4 Pull Mode

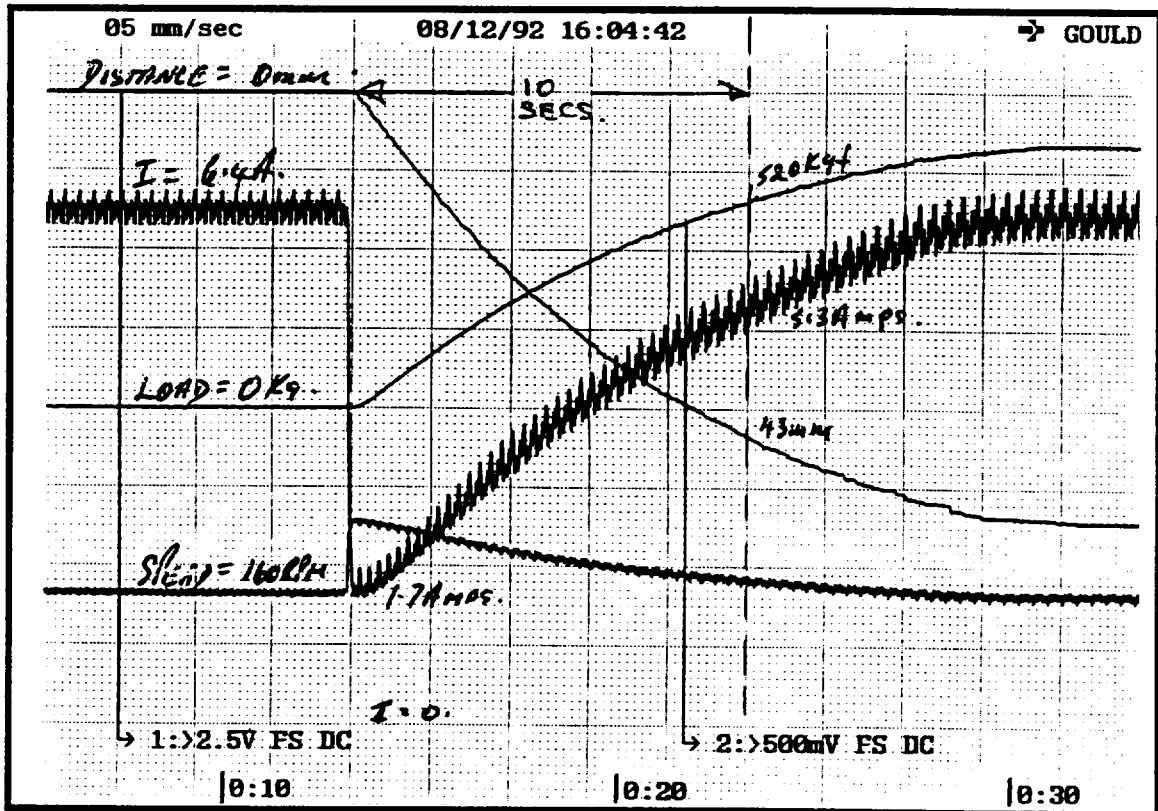


Figure 17. Unit No. 5 Pull Mode